Science Discovery Computers
2026, Vol. 01, No. 2, pp. 80–91
https://doi.org/10.11648/j.sdcomput.20260102.12

SciencePG
Science Publishing Group

Research Article

A Fractional-Order Tumor-Immune-Healthy Tissue Interaction Model: Mathematical Analysis and Numerical Investigation Using the Atangana-Baleanu Derivative

Gizachew Tirite Gellow *

Department of Applied Mathematics, Debre Tabor Universty, Debre Tabor, Ethiopia

Abstract

Tumor progression is governed by nonlinear interactions among malignant cells, immune effector cells, and the surrounding healthy tissue. Such interactions are influenced by previous biological states, including accumulated immune stimulation, tissue damage, and cellular adaptation. Conventional integer-order models describe the instantaneous rate of change but do not explicitly represent this history dependence. In this work, a fractional-order tumor–immune–healthy tissue model is formulated using the Atangana–Baleanu Caputo (ABC) fractional derivative, whose nonsingular Mittag–Leffler kernel provides a nonlocal representation of biological memory. The model consists of three interacting populations: tumor cells, immune effector cells, and healthy tissue. Tumor proliferation is represented by logistic growth, immune-mediated tumor elimination and immune suppression are incorporated through nonlinear interaction terms, and healthy tissue regeneration is balanced against tumor-induced damage. The model is first analyzed mathematically. Under explicit regularity and parameter assumptions, local existence and uniqueness of solutions are established by a fixed-point argument. Positivity is obtained from the vector field on the boundary of the nonnegative orthant, and boundedness follows from comparison estimates. The fractional formulation is then converted into its equivalent Volterra integral equation and a history-weighted product-integration discretization with an implicit correction is implemented for numerical computation. Numerical illustrations are used to examine the effect of fractional order on tumor, immune, and healthy-tissue trajectories. The results indicate that decreasing the fractional order changes the transient response and introduces a stronger dependence on previous states, whereas the integer-order case is recovered at $\alpha = 1$. The study therefore provides a mathematically consistent framework for examining memory-dependent tumor dynamics and identifies directions for subsequent calibration with clinical or experimental data.

Keywords

Fractional Calculus, Atangana-Baleanu Caputo Derivative, Tumor-immune Interaction, Healthy Tissue, Mathematical Biology, Memory Effects, Fractional Differential Equations

1. Introduction

Cancer involves coupled interactions among malignant cells, immune cells, and surrounding tissue. Tumor growth and immune surveillance occur on multiple time scales and can modify the local tissue environment. Mathematical models provide a useful framework for separating these mechanisms and examining their combined dynamics.

Ordinary differential-equation models have been central to the mathematical study of tumor–immune dynamics. The classical

*Correspondence: Gizachew Tirite Gellow (gellowgizachewtirite@gmail.com)

Received: 11 July 2026; **Accepted:** 22 August 2026; **Published:** 3 November 2026

Copyright: © The Author(s), 2026. Published by Science Publishing Group. This is an **Open Access** article, distributed under the terms of the Creative Commons Attribution 4.0 License (http://creativecommons.org/licenses/by/4.0/), which permits unrestricted use, distribution and reproduction in any medium, provided the original work is properly cited.

model of Kuznetsov et al. [1] demonstrated that nonlinear interactions between tumor and immune populations can produce qualitatively different regimes, including tumor elimination and tumor persistence. Kirschner and Panetta [2] subsequently incorporated immune-mediated treatment mechanisms and showed how mathematical models can be used to investigate therapeutic strategies. More broadly, mathematical biology has established that nonlinear feedback, saturation, carrying capacities, and competition can strongly influence the long-term behavior of biological populations [3–5].

Although integer-order models are valuable, they generally describe the instantaneous derivative of a state variable. In many biological systems, however, the current response is not determined exclusively by the present state. Immune activation can reflect previous exposure to tumor antigens, tissue repair can depend on accumulated damage, and cellular adaptation can exhibit persistence over time. These effects are naturally associated with memory and hereditary behavior. Fractional calculus provides a mathematical language for incorporating such history dependence because fractional derivatives are nonlocal operators: the derivative at the present time depends on values of the state over an interval of previous times [6–9].

Several fractional operators have been proposed for biological and physical applications. The Atangana–Baleanu (AB) family is particularly attractive because it employs a nonsingular Mittag–Leffler kernel [10]. Unlike a power-law kernel with a singularity at the origin, the AB kernel remains finite at zero while retaining nonlocal memory. The corresponding Atangana–Baleanu Caputo derivative is convenient for initial-value problems because initial conditions can be expressed in terms of classical integer-order values. Theoretical and numerical developments for fractional differential equations have made it possible to combine these operators with nonlinear biological models [11–15].

Fractional tumor models have already been investigated from several perspectives. Mekkaoui and Atangana [16] studied tumor–immune interactions using fractional and fractional-fractal operators. Other studies have considered fractional cancer–immune models with numerical schemes and attractor analysis [17]. More recent work has explored fractional tumor–immune dynamics in connection with stability, control, synchronization, and numerical optimization [18]. Recent ABC studies have also strengthened the mathematical treatment of existence, uniqueness, stability, and numerical approximation for fractional dynamical systems [15, 19]. These contributions demonstrate the potential value of fractional modeling, but they also highlight the need for models that combine a clear biological interpretation with explicit mathematical conditions and a reproducible numerical formulation.

The present study considers three coupled populations: tumor cells, immune effector cells, and healthy tissue. Including healthy tissue introduces a feedback between tumor burden, tissue damage, and regeneration that is absent from two-population models.

The objective is to establish a mathematically controlled framework in which the memory parameter can be varied. The fractional formulation is treated as a modeling hypothesis that requires calibration or validation before predictive biological conclusions are drawn.

The main contributions are fourfold. First, a fractional tumor–immune–healthy tissue model is formulated with the ABC derivative. Second, explicit sufficient assumptions are stated for local existence and uniqueness and for invariance of the nonnegative region. Third, boundedness conditions are derived from comparison arguments rather than asserted without parameter restrictions. Fourth, the ABC integral representation is used to define a reproducible numerical procedure for exploring the role of the fractional order.

The remainder of the paper is organized as follows. Section 2 introduces the Mittag–Leffler function and the AB operators used throughout the analysis. Section 3 formulates the biological model and explains the meaning of each term. Section 4 establishes existence, uniqueness, positivity, and boundedness. Section 5 describes the numerical discretization and presents illustrative simulations, including a comparison of fractional and integer-order responses. Section 6 discusses the implications and limitations of the results, and Section 7 summarizes the principal conclusions.

2. Fractional Calculus Preliminaries

This section collects the definitions required for the proposed model. Throughout the paper, $0 < \alpha \leq 1$ denotes the fractional order. The case $\alpha = 1$ corresponds to the classical first-order model, whereas values below one introduce nonlocal memory.

2.1. Mittag-Leffler Function

Definition 2.1. For $\alpha > 0$, the one-parameter Mittag–Leffler function is defined by

$$E_\alpha(z) = \sum_{k=0}^{\infty} \frac{z^k}{\Gamma(\alpha k + 1)}. \tag{1}$$

For $\alpha = 1$, $E_1(z) = e^z$.

The Mittag–Leffler function plays in fractional systems a role analogous to that played by the exponential function in many classical systems. Its appearance in the AB kernel allows

past states to contribute to the current derivative without introducing the power-law singularity of several other fractional kernels [12].

2.2. Atangana–Baleanu Fractional Integral

Definition 2.2. Let f be continuous on $[0,T]$ and let $0 < \alpha < 1$. The Atangana–Baleanu fractional integral in the Caputo setting is defined by

$$ {}^{AB}I_t^{\alpha} f(t) = \frac{1-\alpha}{B(\alpha)} f(t) + \frac{\alpha}{B(\alpha)\Gamma(\alpha)} \int_0^t (t-\tau)^{\alpha-1} f(\tau)\, d\tau, \quad (2) $$

where $B(\alpha)$ is a normalization function satisfying $B(0) = B(1) = 1$.

The operator contains a local contribution proportional to $1-\alpha$ and a nonlocal integral contribution proportional to α. Consequently, the model interpolates between local and history-dependent descriptions as the order changes. The precise interpretation of the fractional order depends on the application and should not be identified with a universal biological time scale without parameter estimation.

2.3. Atangana–Baleanu Caputo Derivative

Definition 2.3. For $f \in C^1([0,T])$ and $0 < \alpha < 1$, the Atangana–Baleanu Caputo derivative is

$$ {}^{ABC}D_t^{\alpha} f(t) = \frac{B(\alpha)}{1-\alpha} \int_0^t f'(\tau) E_{\alpha}\left[-\frac{\alpha}{1-\alpha}(t-\tau)^{\alpha}\right] d\tau. \quad (3) $$

At $\alpha = 1$, the corresponding classical first-order derivative is recovered in the limiting formulation.

The nonsingular kernel is useful when the modeled process has a finite instantaneous response but retains memory of previous states. In the tumor application, the operator does not specify a particular biological mechanism by itself. Instead, it provides a mathematical representation of memory that can subsequently be tested against data.

2.4. Equivalent Integral Equation

Consider the ABC initial-value problem

$$ {}^{ABC}D_t^{\alpha} x(t) = F(t, x(t)), \qquad x(0) = x_0. \quad (4) $$

Under the regularity assumptions required for the AB operators, the problem can be represented by a Volterra-type integral equation of the form

$$ x(t) = x_0 + {}^{AB}I_t^{\alpha} F(t, x(t)). \quad (5) $$

This representation is central to both the existence argument and the numerical approximation used later.

Lemma 2.4. *Suppose that $F : [0,T]\times\mathbb{R}^n \to \mathbb{R}^n$ is continuous and locally Lipschitz in its second argument. Then the integral operator associated with (5) is continuous on $C([0,T],\mathbb{R}^n)$ and is a contraction on a sufficiently short interval whenever its Lipschitz constant and the interval length satisfy the corresponding contraction bound.*

Proof. Continuity follows from the continuity of F and the boundedness of the AB integral operator on a finite interval. If F is Lipschitz with constant L, the difference of the images of two functions is bounded by the sum of the local AB contribution and the weakly singular Volterra contribution. Both terms are proportional to the norm of the difference, and their coefficient tends to zero with the length of the time interval. Thus a sufficiently short interval makes the operator contractive, and Banach's fixed-point theorem applies. □

3. Model Formulation

3.1. Biological Assumptions

The model is constructed under the following assumptions.

1) Tumor cells proliferate logistically because available resources and space are limited.
2) Immune effector cells remove tumor cells through a mass-action interaction.
3) Tumor presence stimulates immune activity, while tumor–immune interaction also contains a suppressive component.
4) Tumor cells damage healthy tissue through a mass-action interaction.
5) Healthy tissue regenerates logistically in the absence of tumor-induced damage.
6) The memory associated with the three biological populations is represented by a common fractional order α.
7) All state variables and parameters are nonnegative, and sufficient parameter restrictions are imposed where required for boundedness.

3.2. State Variables

Let $T(t)$, $I(t)$, and $H(t)$ denote, respectively, tumor cells, immune effector cells, and healthy tissue at time t. Their definitions and biological roles are summarized in Table 1. The state vector is

$$ X(t) = \big(T(t), I(t), H(t)\big)^{\top}. \quad (6) $$

Table 1. State variables of the model.

Symbol	Description	Interpretation
$T(t)$	Tumor population	malignant-cell burden
$I(t)$	Immune population	immune effector-cell level
$H(t)$	Healthy tissue	viable surrounding tissue

3.3. Fractional Tumor–Immune–Healthy Tissue System

The proposed model is

$$\begin{aligned} {}^{ABC}D_t^{\alpha}T(t) &= r_T T\left(1-\frac{T}{K_T}\right)-\beta TI-\gamma TH,\\ {}^{ABC}D_t^{\alpha}I(t) &= s+\eta TI-\mu I-\delta TI,\\ {}^{ABC}D_t^{\alpha}H(t) &= r_H H\left(1-\frac{H}{K_H}\right)-\rho TH, \end{aligned} \tag{7}$$

with initial conditions

$$T(0)=T_0\geq 0, \qquad I(0)=I_0\geq 0, \qquad H(0)=H_0\geq 0. \tag{8}$$

Table 2 gives the model parameters and their biological interpretation. The parameter r_T is the intrinsic tumor growth rate and K_T is its carrying capacity. The coefficient β measures immune-mediated tumor elimination, while γ represents tumor-associated damage to healthy tissue. The constant s denotes basal immune recruitment. The parameter η describes tumor-associated immune stimulation, μ is the natural immune loss rate, and δ is the tumor-associated suppressive coefficient. Finally, r_H and K_H are the regeneration rate and carrying capacity of healthy tissue, respectively, and ρ measures tumor-induced tissue damage.

Table 2. Model parameters and biological interpretation.

Parameter	Biological interpretation	Nonnegativity
r_T	Intrinsic tumor proliferation rate	$r_T \geq 0$
K_T	Tumor carrying capacity	$K_T > 0$
β	Immune-mediated tumor elimination coefficient	$\beta \geq 0$
γ	Tumor-associated healthy-tissue damage coefficient	$\gamma \geq 0$
s	Basal immune recruitment rate	$s \geq 0$
η	Tumor-associated immune stimulation coefficient	$\eta \geq 0$
μ	Natural immune loss rate	$\mu > 0$
δ	Tumor-associated immune suppression coefficient	$\delta \geq 0$
r_H	Healthy-tissue regeneration rate	$r_H \geq 0$
K_H	Healthy-tissue carrying capacity	$K_H > 0$
ρ	Tumor-induced tissue damage coefficient	$\rho \geq 0$
α	Fractional order	$0 < \alpha \leq 1$

3.4. Interpretation of the Interaction Terms

The tumor equation contains four mechanisms. Logistic growth allows tumor expansion when the population is small and limits growth as the carrying capacity is approached. The term $-\beta TI$ represents direct immune-mediated killing. The term $-\gamma TH$ represents tumor-associated interaction with healthy tissue; it can be interpreted as a phenomenological loss of tumor viability associated with contact with or competition involving healthy tissue. This term also contributes to the reduction of the healthy compartment through the third equation.

The immune equation contains basal recruitment s and tumor-associated stimulation ηTI. The natural loss $-\mu I$ prevents indefinite accumulation of immune cells. The term $-\delta TI$ represents tumor-induced immune suppression. Thus the net tumor–immune contribution to the immune equation is $(\eta-\delta)TI$. In particular, when $\delta > \eta$, the net interaction is suppressive; when $\eta > \delta$, stimulation dominates. This distinction becomes important for the boundedness condition established below.

The healthy-tissue equation combines regeneration with tumor-induced damage. In the absence of tumor cells, the healthy population follows logistic regeneration and approaches K_H for positive initial data. When $T > 0$, the term $-\rho TH$ reduces healthy tissue. The model therefore permits tumor persistence to be associated with progressive tissue loss, while regeneration can oppose that loss.

3.5. Dimensionless Considerations

For numerical work, populations can be normalized by their respective carrying capacities, for example $x = T/K_T$ and $h = H/K_H$, while immune cells can be scaled by a reference immune level. Such nondimensionalization reduces the number of independent scales and can facilitate sensitivity analysis. In the present manuscript the dimensional symbols are retained to keep the biological interpretation transparent. Consequently, the numerical values used in an illustrative simulation should be interpreted as normalized model units unless they have been estimated from a specified experimental data set.

4. Mathematical Analysis

Let

$$F(X) = \begin{pmatrix} r_T T(1 - T/K_T) - \beta TI - \gamma TH \\ s + (\eta - \delta)TI - \mu I \\ r_H H(1 - H/K_H) - \rho TH \end{pmatrix}. \tag{9}$$

The right-hand side is polynomial and therefore locally Lipschitz on $\mathbb{R}^3$. This observation provides the basis for the local well-posedness result.

4.1. Local Existence and Uniqueness

Theorem 4.1. *For nonnegative initial data satisfying (8) and nonnegative finite parameters, system (7) has a unique local solution on an interval* $[0, T_*]$, *with* $T_* > 0$.

Proof. Because each component of F is a polynomial in (T, I, H), F is continuous and locally Lipschitz on every bounded subset of $\mathbb{R}^3$. Let Ω_R be a closed ball containing the initial vector X_0. On Ω_R, there exists $L_R > 0$ such that $\|F(X) - F(Y)\| \le L_R\|X - Y\|$. The integral formulation associated with the ABC derivative defines an operator $\mathcal{T}$ on $C([0, T_*], \Omega_R)$. The local and Volterra components of the AB integral are bounded by constants times $\|F(X) - F(Y)\|$. Hence

$$\|\mathcal{T}X - \mathcal{T}Y\|_\infty \le q(T_*)\|X - Y\|_\infty, \tag{10}$$

where $q(T_*) < 1$ for sufficiently small T_*. The operator is therefore a contraction. Banach's fixed-point theorem yields a unique fixed point, which is the unique local solution of the fractional system. □

4.2. Positive Invariance

Theorem 4.2. *If* $T_0, I_0, H_0 \ge 0$, *then the nonnegative orthant* $\mathbb{R}^3_+$ *is positively invariant for system (7).*

Proof. On the boundary $T = 0$ with $I, H \ge 0$, the tumor component satisfies $F_1(0, I, H) = 0$. On $I = 0$, one has $F_2(T, 0, H) = s \ge 0$. On $H = 0$, one has $F_3(T, I, 0) = 0$. Thus no component has an outward-pointing vector field on its corresponding coordinate boundary. The standard invariant-region argument for fractional Volterra systems then prevents a nonnegative solution from crossing any coordinate plane into the negative region. Hence $T(t), I(t), H(t) \ge 0$ throughout the interval of existence. □

Remark 4.3. The positivity result is structural and does not require a particular numerical method. A numerical algorithm used for simulation should nevertheless be checked for preservation of nonnegativity, especially for large time steps.

4.3. Boundedness

The nonlinear interaction in the immune equation requires a parameter restriction if a simple global bound is to be obtained. We therefore state the sufficient condition explicitly rather than assuming boundedness automatically.

Assumption 4.4. The tumor-associated immune suppression is at least as strong as tumor-associated immune stimulation, that is,

$$\delta \ge \eta. \tag{11}$$

Theorem 4.5. *Under Assumption (11), nonnegative solutions of (7) are bounded for all times for which the solution exists. In particular, comparison with scalar fractional logistic equations yields finite upper bounds for* $T(t)$ *and* $H(t)$, *while* $I(t)$ *is bounded by the scalar linear inequality* ${}^{ABC}D_t^\alpha I \le s - \mu I$.

Proof. Since all interaction coefficients are nonnegative,

$${}^{ABC}D_t^\alpha T \le r_T T\left(1 - \frac{T}{K_T}\right). \tag{12}$$

By the fractional comparison principle, T is bounded above by the solution of the corresponding scalar fractional logistic equation. Consequently, T cannot grow without bound. Similarly,

$${}^{ABC}D_t^\alpha H \le r_H H\left(1 - \frac{H}{K_H}\right), \tag{13}$$

so H is bounded above by a fractional logistic comparison solution.

For the immune population, Assumption (11) gives $(\eta - \delta)TI \le 0$. Therefore,

$${}^{ABC}D_t^\alpha I \le s - \mu I. \tag{14}$$

The scalar comparison equation has a finite equilibrium level s/μ, and hence $I(t)$ is bounded by a finite function determined

by I_0, s, and μ. Since all three components are nonnegative and bounded, the solution remains in a bounded feasible region and can be continued globally. □

4.4. Feasible Region

A convenient invariant set is therefore

$$\Omega = \{(T, I, H) \in \mathbb{R}^3_+ : 0 \le T \le M_T,\ 0 \le I \le M_I,\ 0 \le H \le M_H\} \quad (15)$$

where M_T, M_I, and M_H are finite comparison bounds. The exact values depend on the initial conditions and parameters. The set Ω is the appropriate domain for subsequent numerical investigation.

4.5. Equilibria and the Classical Limit

At an equilibrium $X^* = (T^*, I^*, H^*)$, the right-hand side of (7) vanishes. Thus

$$0 = r_T T^*(1 - T^*/K_T) - \beta T^* I^* - \gamma T^* H^*, \quad (16)$$

$$0 = s + (\eta - \delta) T^* I^* - \mu I^*, \quad (17)$$

$$0 = r_H H^*(1 - H^*/K_H) - \rho T^* H^*. \quad (18)$$

These algebraic relations show how tumor burden, immune response, and tissue condition are coupled at steady state. In particular, if $s > 0$, a tumor-free equilibrium must satisfy $T^* = 0$, $I^* = s/\mu$, and $H^* = K_H$. Whether this equilibrium is locally stable depends on the parameter combination governing tumor invasion and is not determined by the existence calculation alone.

When $\alpha \to 1$, the memory operator approaches the classical derivative and the system reduces formally to

$$\dot{T} = r_T T(1 - T/K_T) - \beta T I - \gamma T H, \quad (19)$$

$$\dot{I} = s + (\eta - \delta) T I - \mu I, \quad (20)$$

$$\dot{H} = r_H H(1 - H/K_H) - \rho T H. \quad (21)$$

Thus the integer-order system is included as the limiting reference case.

5. Numerical Method and Illustrative Results

5.1. Numerical Formulation

The numerical computation is based on the equivalent integral representation of the ABC system. Let $t_n = n\Delta t$, $n = 0, 1, \ldots, N$, with $N\Delta t = T_f$. For the vector state $X = (T, I, H)^{\mathsf{T}}$ and nonlinear vector field $F(X)$, the model is written as

$$X(t) = X_0 + \frac{1-\alpha}{B(\alpha)} F(X(t)) + \frac{\alpha}{B(\alpha)\Gamma(\alpha)} \int_0^t (t-\tau)^{\alpha-1} F(X(\tau))\, d\tau. \quad (22)$$

The numerical scheme used in the present study approximates the history integral by piecewise-constant product integration. On the interval $[t_j, t_{j+1}]$, the nonlinear term is represented by $F_j = F(X_j)$. Therefore, at t_n the history contribution is approximated by

$$\int_0^{t_n} (t_n - \tau)^{\alpha-1} F(X(\tau))\, d\tau \approx \sum_{j=0}^{n-1} w_{n,j}^{(\alpha)} F_j, \quad (23)$$

where

$$w_{n,j}^{(\alpha)} = \frac{(t_n - t_j)^{\alpha} - (t_n - t_{j+1})^{\alpha}}{\alpha}. \quad (24)$$

These weights retain contributions from all previous time intervals and therefore explicitly preserve the nonlocal memory of the ABC operator. Numerical approximation of ABC derivatives requires such history-dependent treatment; methods based on the ABC kernel have been developed and analyzed in the fractional numerical-analysis literature [11, 20–22].

At each new time level, an explicit predictor is first formed using F_{n-1}. The predicted state is then used to initialize an implicit correction. In compact form, the corrected state is obtained from

$$X_n = X_0 + \frac{1-\alpha}{B(\alpha)} F(X_n) + \frac{\alpha}{B(\alpha)\Gamma(\alpha)} \left[\sum_{j=0}^{n-2} w_{n,j}^{(\alpha)} F_j + w_{n,n-1}^{(\alpha)} F(X_n) \right], \quad (25)$$

with the first iterate supplied by the predictor. A nonlinear root solve is used for the three coupled equations at each time level; this history-dependent treatment is consistent with recent ABC numerical developments that emphasize explicit memory contributions, stability, and convergence verification [20–22], and negative numerical values, if produced only at the level of round-off error, are projected to zero. The computation uses $T_f = 10$ and $N = 500$, corresponding to $\Delta t = 0.02$. Fractional orders $\alpha = 0.6$, 0.8, and 1 are considered.

To assess numerical robustness, the computation for $\alpha = 0.8$

was repeated with $N = 125, 250, 500$, and 1000. The terminal values changed progressively less as the step size was refined, as shown in Table 3. This refinement check is not a formal proof of convergence order; rather, it provides a practical verification that the reported trajectories are not artifacts of a single coarse time grid.

Table 3. *Time-step refinement for the illustrative simulation with* $\alpha = 0.8$.

N	Δt	$T(10)$	$I(10)$	$H(10)$
125	0.080	4.7266	0.9971	7.5665
250	0.040	4.7305	0.9984	7.5628
500	0.020	4.7325	0.9990	7.5609
1000	0.010	4.7335	0.9993	7.5599

5.2. Illustrative Parameter Set

The original manuscript contained unspecified entries in the parameter table. To avoid presenting unsupported biological estimates as measured quantities, the present version treats the following values as a *dimensionless illustrative parameter set*. They are intended to demonstrate the numerical behavior of the model, not to represent a calibrated patient population.

Table 4. *Illustrative dimensionless parameter set used for qualitative numerical demonstration.*

r_T	K_T	β	γ	s	η	μ	δ	r_H	K_H	ρ
0.60	10	0.03	0.02	0.40	0.01	0.50	0.02	0.40	10	0.03

The complete illustrative parameter vector is reported in Table 4. The values satisfy $\delta \geq \eta$, so the sufficient boundedness condition is respected. The initial state for the illustrative trajectories is chosen as

$$(T_0, I_0, H_0) = (1, 3, 9), \tag{26}$$

and simulations are considered on $0 \leq t \leq 10$. Fractional orders $\alpha = 0.6, 0.8$, and 1 are used to illustrate increasing memory and the classical reference case. Because these values are not fitted to clinical observations, the numerical figures should be read as structural illustrations rather than quantitative predictions.

5.3. Interaction Structure

Figure 1 summarizes the biological feedbacks. Tumor cells grow intrinsically and interact with immune and healthy-tissue populations. Immune cells are recruited basally and stimulated by tumor presence but experience natural loss and tumor-associated suppression. Healthy tissue regenerates but is reduced by tumor-induced damage.

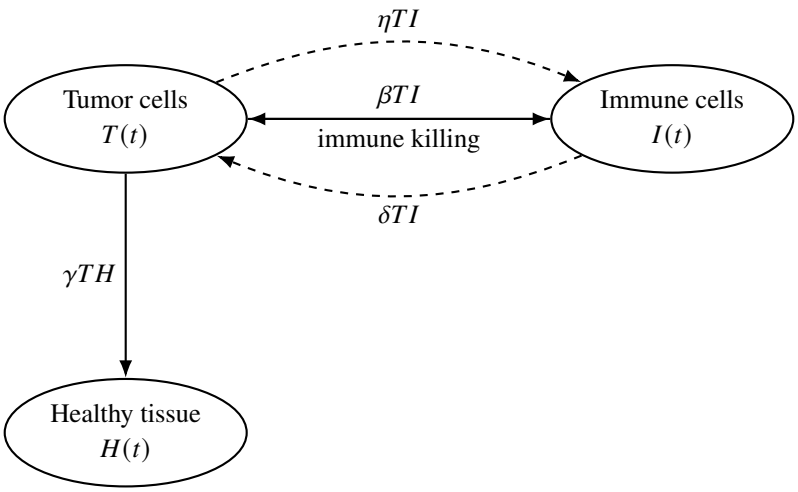


Figure 1. *Schematic representation of the three-population interaction structure.*

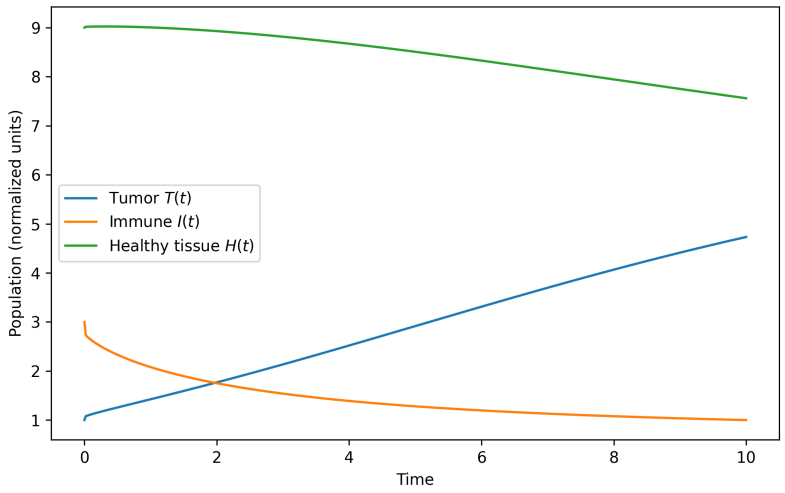


Figure 2. *Numerically computed trajectories of tumor, immune, and healthy-tissue populations for the illustrative parameter set with* $\alpha = 0.8$, $N = 500$, *and* $\Delta t = 0.02$.

Figure 2 provides the corresponding computed trajectories. The figure emphasizes an important qualitative feature: tumor growth does not occur independently of the immune and healthy compartments. An increase in tumor burden stimulates the immune component, but the same tumor burden also damages healthy tissue. The resulting trajectories are therefore determined by the balance of several nonlinear mechanisms rather than by tumor proliferation alone.

5.4. Effect of Fractional Order

The fractional order controls the relative contribution of historical states. Figure 3 illustrates the qualitative effect of choosing $\alpha = 0.6$, 0.8, and 1. For lower α, the system retains a stronger memory contribution, and the transient trajectory differs from the integer-order case. The important point is not that a lower order necessarily produces slower or faster tumor growth in every parameter regime; rather, the order changes the weighting of the history term and can therefore alter the transient and long-term response depending on the parameter set.

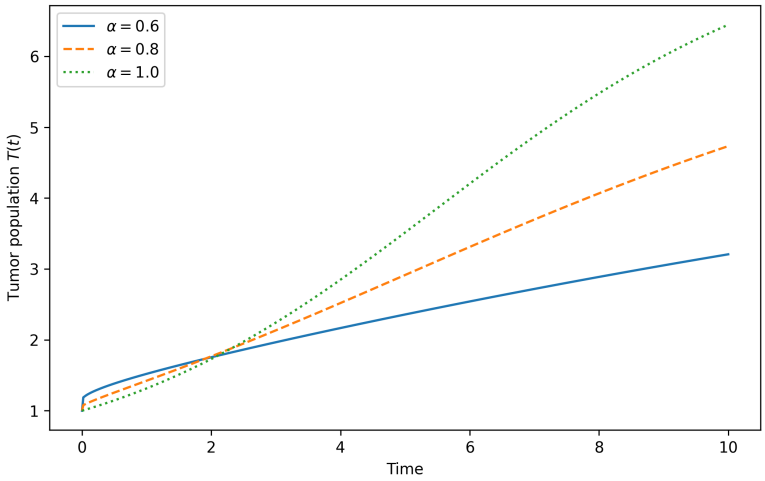


Figure 3. *Numerically computed tumor trajectories for* $\alpha = 0.6$, 0.8, *and* 1 *using the same illustrative parameter set and time grid. The integer-order case is the classical reference.*

The separation among the curves illustrates why the fractional order can be used as an additional modeling parameter. In a calibrated application, α could be estimated jointly with biological parameters and compared with an integer-order model using an appropriate goodness-of-fit criterion. Without such data, however, the present comparison is descriptive rather than inferential.

5.5. Fractional versus Integer-Order Formulation

Figure 4 compares one fractional case with the classical limit. The fractional response differs because the derivative at a given time incorporates information from earlier states. The difference should not be interpreted as evidence that the fractional model is universally more accurate. Instead, it demonstrates the additional dynamical degree of freedom introduced by the memory operator.

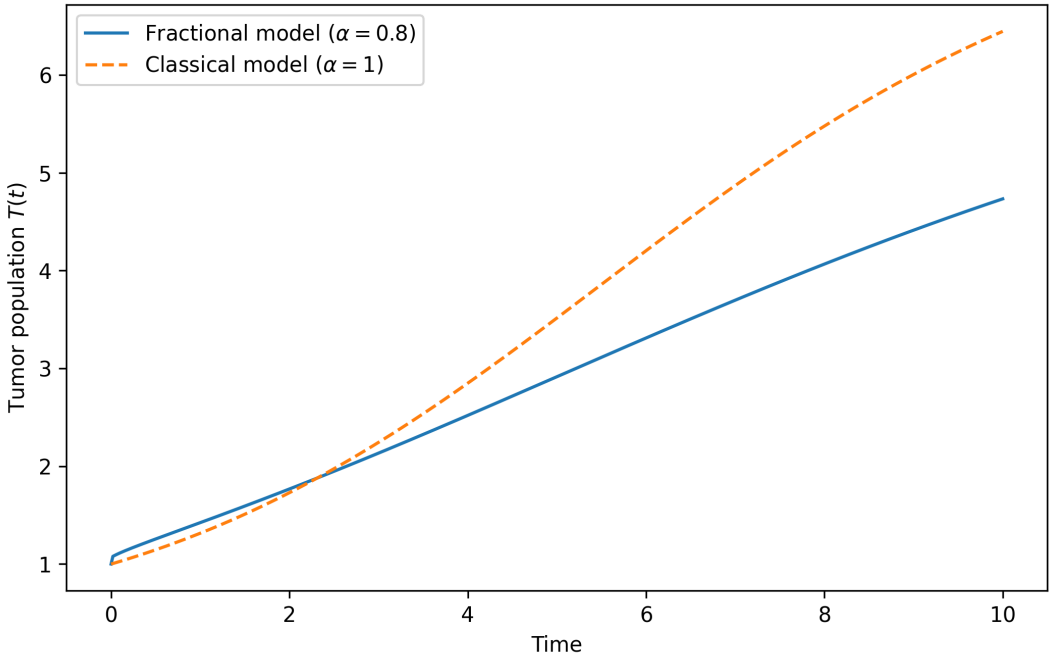


Figure 4. *Numerical comparison between the fractional-order model with $\alpha = 0.8$ and the classical model with $\alpha = 1$ under identical initial conditions and parameters.*

5.6. Discussion of the Numerical Findings

The numerical illustrations support three observations. First, the model generates coupled trajectories rather than independent population curves. Tumor expansion changes the immune response and damages healthy tissue, while changes in immune and tissue populations feed back into tumor dynamics. Second, fractional order modifies the transient behavior. Because the ABC derivative contains a history integral, the state at time t depends on the preceding trajectory and not solely on the instantaneous population values. Third, the integer-order system is recovered as the reference limit, making it possible to investigate whether a fractional formulation provides a statistically or mechanistically better description when observations become available.

The simulations demonstrate computational behavior but do not constitute clinical validation. A subsequent data-based study should estimate the parameters and fractional order, quantify uncertainty, and test predictions on observations not used for calibration.

Sensitivity analysis should examine r_T, β, μ, δ, and α. Global methods such as Latin-hypercube sampling and partial-rank correlation could identify dominant sources of uncertainty and assess whether α is identifiable independently of conventional parameters.

6. Limitations and Future Directions

The model is a low-dimensional representation of a complex tumor microenvironment containing multiple cell types, signaling pathways, and spatial heterogeneity. A common fractional order is also assumed for all compartments, whereas different processes may exhibit different memory characteristics.

The numerical parameter set is illustrative rather than clinically calibrated. Future work should use longitudinal tumor, immune, and tissue measurements and estimate conventional parameters and α by optimization or Bayesian inference.

The model is deterministic and spatially homogeneous. Reaction–diffusion or advection–diffusion extensions could represent invasion, nutrient gradients, immune migration, and interactions between memory and spatial transport.

Therapeutic interventions are not included. Future extensions could incorporate chemotherapy, radiotherapy, or immunotherapy as control inputs and investigate optimal treatment while preserving healthy tissue.

7. Conclusion

A fractional-order tumor–immune–healthy tissue interaction model was developed using the Atangana–Baleanu Caputo derivative with a nonsingular Mittag–Leffler kernel. The model combines logistic tumor growth, immune recruitment and tumor-associated stimulation and suppression, healthy-tissue regeneration, and tumor-induced tissue damage. The formulation provides a compact framework for studying how biological memory may influence the coupled evolution of malignant, immune, and healthy populations.

The mathematical analysis established local existence and uniqueness under the standard local Lipschitz condition associated with the polynomial vector field. Positivity was obtained from the boundary behavior of the model, ensuring that population variables remain biologically meaningful. A sufficient condition, $\delta \geq \eta$, was explicitly imposed to obtain a simple boundedness result for the immune component and, together with logistic comparison estimates, boundedness of the complete system. Stating this condition explicitly strengthens the mathematical consistency of the model compared with an unconditional boundedness assertion.

The equivalent AB integral formulation was used to describe a predictor–corrector numerical strategy that preserves the nonlocal history contribution. Illustrative simulations showed how different fractional orders can modify the transient tumor response and how the fractional formulation differs from the classical integer-order reference. These numerical results should be interpreted as qualitative demonstrations because the parameter set has not been fitted to clinical or experimental observations.

The principal value of the framework is therefore methodological: it combines a biologically interpretable three-population model with a memory operator and explicit mathematical conditions. Future research should focus on parameter estimation, uncertainty and sensitivity analysis, comparison with integer-order alternatives using real observations, multi-order memory, spatial effects, and therapeutic control. These developments are necessary before the model can be used for quantitative prediction or clinical decision support.

Abbreviations

ABC	Atangana–Baleanu Caputo
AB	Atangana Baleanu

Acknowledgments

The author acknowledges Debre Tabor University for providing an academic environment that supports research and scientific development.

Author Contributions

Gizachew Tirite Gellow: Conceptualization, Formal Analysis, Methodology, Writing – original draft, Writing – review & editing

Data Availability Statement

No experimental or clinical datasets were used in this study. The illustrative trajectories are generated from the mathematical formulation described in the manuscript. A reproducible computational implementation can be prepared from the stated equations, parameter set, initial conditions, and numerical procedure.

Conflicts of Interest

The author declares that there is no conflict of interest regarding the publication of this paper.

References

[1] V. A. Kuznetsov, I. A. Makalkin, M. A. Taylor and A. S. Perelson, Nonlinear dynamics of immunogenic tumors: Parameter estimation and global bifurcation analysis, *Bulletin of Mathematical Biology*, 56, 295–321, 1994.

[2] D. Kirschner and J. C. Panetta, Modeling immunotherapy of the tumor–immune interaction, *Journal of Mathematical Biology*, 37, 235–252, 1998. https://doi.org/10.1007/s002850050127

[3] J. D. Murray, *Mathematical Biology I: An Introduction*, Springer, New York, 2002. https://doi.org/10.1007/b98868

[4] Leah Edelstein-Keshet, *Mathematical Models in Biology*, Classics in Applied Mathematics, Vol. 46, SIAM, Philadelphia, 2005. https://doi.org/10.1137/1.9780898719147

[5] A. S. Perelson, "Modelling viral and immune system dynamics," *Nature Reviews Immunology*, vol. 2, no. 1, pp. 28–36, 2002. https://doi.org/10.1038/nri700

[6] I. Podlubny, *Fractional Differential Equations*, Mathematics in Science and Engineering, Vol. 198, Academic Press, San Diego, 1999. https://doi.org/10.1016/S0076-5392(99)80065-2

[7] A. A. Kilbas, H. M. Srivastava, and J. J. Trujillo, *Theory and Applications of Fractional Differential Equations*, Elsevier Science (North-Holland Mathematics Studies, Vol. 204), Amsterdam, 2006. https://doi.org/10.1016/S0304-0208(06)80001-9

[8] K. Diethelm, *The Analysis of Fractional Differential Equations*, Lecture Notes in Mathematics, Vol. 2004, Springer, Berlin, 2010. https://doi.org/10.1007/978-3-642-14574-2

[9] F. Mainardi, *Fractional Calculus and Waves in Linear Viscoelasticity*, Imperial College Press, London, 2010. https://doi.org/10.1142/p639

[10] A. Atangana and D. Baleanu, "New fractional derivatives with nonlocal and nonsingular kernel: Theory and application to heat transfer model," *Thermal Science*, vol. 20, no. 2, pp. 763–769, 2016. https://doi.org/10.2298/TSCI160111018A

[11] A. Atangana and K. M. Owolabi, "New numerical approach for fractional differential equations," *Mathematical Modelling of Natural Phenomena*, vol. 13, no. 1, pp. 1–15, 2018. https://doi.org/10.1051/mmnp/2018011

[12] R. Gorenflo, A. A. Kilbas, F. Mainardi, and S. V. Rogosin, *Mittag-Leffler Functions, Related Topics and Applications*, Springer Monographs in Mathematics, Springer, Berlin, 2014. https://doi.org/10.1007/978-3-662-43930-2

[13] R. Hilfer, *Applications of Fractional Calculus in Physics*, World Scientific, Singapore, 2000. https://doi.org/10.1142/9789812817747

[14] S. G. Samko, A. A. Kilbas, and O. I. Marichev, *Fractional Integrals and Derivatives: Theory and Applications*, Gordon and Breach Science Publishers, Amsterdam, 1993. https://doi.org/10.1201/9780203745289

[15] E. A. A. Ziada, Picard and Adomian solutions of nonlinear fractional differential equations system containing Atangana–Baleanu derivative, *Journal of Engineering and Applied Science*, 71, 31, 2024. https://doi.org/10.1186/s44147-024-00361-6

[16] T. Mekkaoui and A. Atangana, "On the modeling of the interaction between tumor growth and the immune system using some new fractional and fractional-fractal operators," *Chaos, Solitons & Fractals*, vol. 137, 109887, 2020. https://doi.org/10.1016/j.chaos.2020.109887

[17] H. Alotaibi, et al., "Numerical solutions and geometric attractors of a fractional model of the cancer-immune based on the Atangana–Baleanu–Caputo derivative and the reproducing kernel scheme," *Chinese Journal of Physics*, vol. 80, pp. 463–483, 2022. https://doi.org/10.1016/j.cjph.2022.01.019

[18] S. R. Aderyani, R. Saadati, F. R. Aderyani, and O. Tunç, "Mathematical modeling of tumor-immune dynamics: stability, control, and synchronization via fractional calculus and numerical optimization," *Scientific Reports*, vol. 15, 29094, 2025. https://doi.org/10.1038/s41598-025-29094-9

[19] A. Abbas, N. Mehmood, M. De la Sen and A. Al-Rawashdeh, Mathematical analysis of dynamical systems involving Atangana–Baleanu piecewise derivative, *Alexandria Engineering Journal*, 120, 438–448, 2025. https://doi.org/10.1016/j.aej.2025.02.028

[20] S. Yadav, R. K. Pandey and A. K. Shukla, Numerical approximations of Atangana–Baleanu Caputo derivative and its appslication, *Chaos, Solitons & Fractals*, 118, 58–64, 2019. https://doi.org/10.1016/j.chaos.2018.11.009

[21] A. Ghafoor, M. Fiaz, K. Shah and T. Abdeljawad, Analysis of nonlinear Burgers equation with time fractional Atangana–Baleanu–Caputo derivative, *Heliyon*, 10(13), e33842, 2024. https://doi.org/10.1016/j.heliyon.2024.e33842

[22] R. Noureen, M. K. Iqbal, M. Asgir, B. Almohsen and M. Azeem, A novel approach to approximate solution of time fractional gas dynamics equation with Atangana–Baleanu derivative, *Alexandria Engineering Journal*, 116, 451–471, 2025. https://doi.org/10.1016/j.aej.2024.11.075